FAILURE PREDICTION OF INJECTION-MOULDED SHORT-FIBRE COMPOSITES: CHARACTERISATION AND PREDICTION FROM COUPONS TO COMPONENTS

Yuki Fujita[1,2,3*], Satoshi Noda[2], Shunta Kimura[2], Junichi Takahashi[2],
Emile S. Greenhalgh[3], Soraia Pimenta[1]

[1] Department of Mechanical Engineering, Imperial College London, South Kensington Campus,
SW7 2AZ London, United Kingdom (y.fujita@imperial.ac.uk)

[2] Polymers R&D Planning and Business Development, Asahi Kasei Corporation,
210-0863, 1-3-1, Yako, Kawasaki, Japan

[3] Department of Aeronautics, Imperial College London, South Kensington Campus,
SW7 2AZ London, United Kingdom

Keywords: Injection moulded composites, Fracture toughness, Coupled finite element analysis, Cohesive zone modelling, Fractography

ABSTRACT

Injection-moulded short-fibre composites are lightweight materials suitable for high-volume applications; however, current simulation methods for these materials cannot yet predict failure accurately. This work proposes a methodology to predict failure of injection-moulded short-glass-fibre reinforced PA66 composite components, based on experimentally measured properties. The material's fracture toughness was characterized for different fibre orientations and environmental conditions, and these values were used as the input for cohesive zone modelling in Finite Element analyses of the subcomponents, coupled with the fibre orientations predicted by an injection-moulding process simulation. The coupled process/structural simulations using cohesive zone modelling presented excellent agreement with the experimental data of the subcomponent tests, highlighting the importance of accounting for the finite fracture toughness of the material to accurately predict the ultimate failure of injection-moulded short-fibre reinforced PA66 composite components.

1 INTRODUCTION

Injection-moulded (IM) short-glass fibre reinforced thermoplastics (SFRPs) have three key advantages over conventional materials: they are lightweight, they have short production cycles, and they can be moulded into complex 3D-shaped components. The injection-moulding process creates a core-shell micro-structure with complex fibre orientation states, as the fibres align along the flow direction in the shell, and along the transverse direction or randomly in the core (as shown in Figure 1). This microstructure leads to anisotropic and heterogeneous mechanical properties and failure modes, which complicates the design of SFRP components.

When designing SFRP components, it is necessary to predict when and where failure will occur. However, existing failure criteria for SFRPs (e.g. based on the Tsai-Hill criterion [1]) underestimate the failure load of components, because they consider failure initiation only and neglect the finite toughness of the material. The objective of this work is therefore to develop a Finite-Element methodology to polyamide 6.6, by accounting for the material's progressive failure.

2 MANUFACTURING

Polyamide 6.6 reinforced by 50% (wt) glass-fibres (PA66-GF50) from Asahi Kasei Corporation was used to injection-mould plates (Figure 1). Dog-bone specimens (based on the geometry of ISO8256) and Compact-Tension (CT) specimens (Figure 2) were machined at several angles from the IM-plates [2]. Subcomponents (Figure 3), representing a simplified geometry of an automotive component, were also manufactured with the same material as used for IM-plates. These samples were kept under dry as moulded (DAM), or conditioned under 50% of relative humidity (RH50, according to ISO1110 [3]).

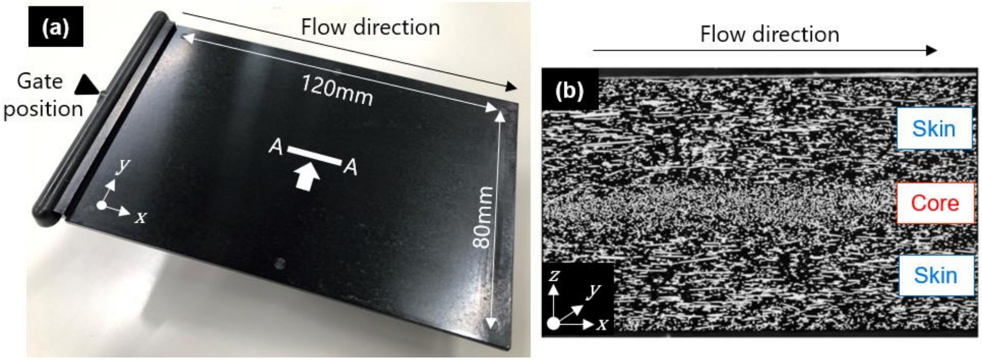

Figure 1: (a) Photograph of an injection-moulded PA66-GF50 plate (2 mm thick along z). The A-A line indicates the *x*-*z* plane, and (b) Cross-sectional optical micrograph across the A-A line [2].

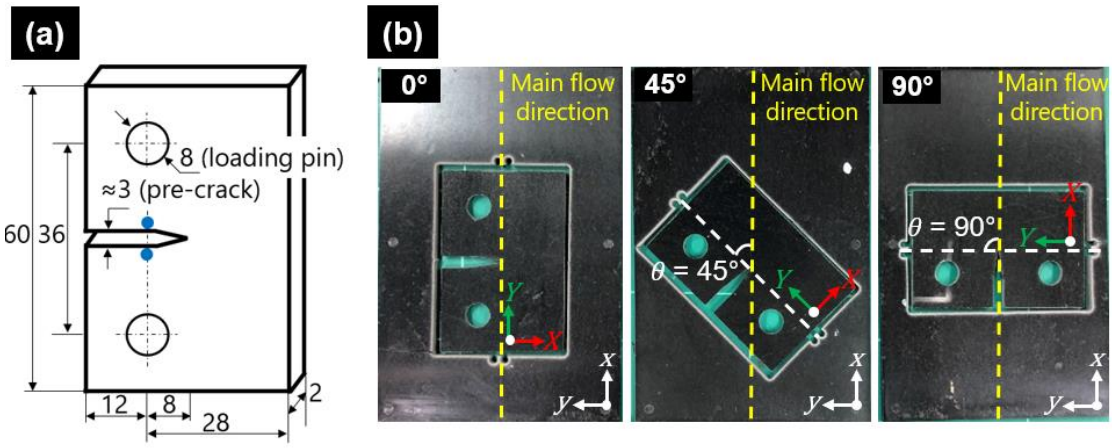

Figure 2: Design of CT specimens: (a) details of the geometry (all dimensions in mm), and (b) definition of the machining angles [2].

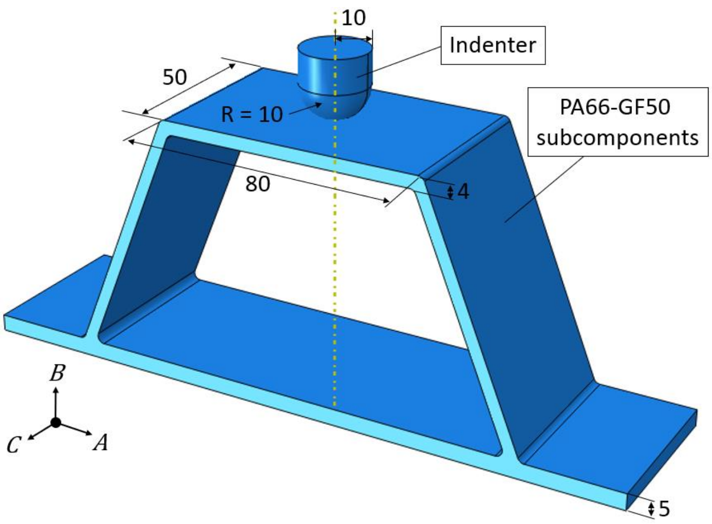

Figure 3: PA66-GF50 subcomponents.

3 CHARACTERISATION OF FRACTURE TOUGHNESS

Tensile CT tests were conducted using CT specimens machined at several angles from the IM plates; all details have been published [2], and are here summarized for completeness. Representative load-displacement curves of CT specimens tested at different machining angles and environmental conditions are shown in Figure 4. All specimens exhibited a stable crack propagation (with a gradual decrease in the load after the peak). The value of the peak load was the highest for the specimens machined at a 0° angle, and progressively decreased with increasing machining angles. The value of peak load decreased with an increase in moisture content or temperature.

These load-displacement curves of CT specimens were transformed to R-curves (using compliance calibration or the J-integral method [2]), and the value of the plateau region in the R-curves were regarded as the overall fracture toughness (or critical strain energy release rate) of the PA66-GF50 material. These fracture toughnesses as a function of machining angles are presented in Figure 5 (a). The fracture toughness was maximum at 0° (i.e. for fracture across the preferential fibre orientation direction), and decreased as the machining angle increased up to 90° (i.e. for fracture along the preferential fibre orientation). Moreover, the fracture toughness increased under hotter/wetter conditions. These fracture toughness plots were transformed to functions of the preferential fibre orientation tensor a_{YY}, as shown in Figure 5 (b) (the procedures are shown in [2]).

The fracture surfaces of CT specimens after testing were observed using scanning electron microscope (SEM) to characterise the damage mechanisms. These representative SEM images (in the shell region) after the tests under 23°C-DAM conditions, for the different machining angles, are shown in Figure 6. Large deformation of the PA66 matrix with good interfacial adhesion was observed in all angles. It was also noted that failure mechanisms in the shell region was dominated by fibre tension in the 0° specimens, then shifting to matrix shear failure in the 45° specimens (where the fibres were preferentially aligned diagonally with respect to the crack faces), and to matrix transverse tension failure in the 90° specimens.

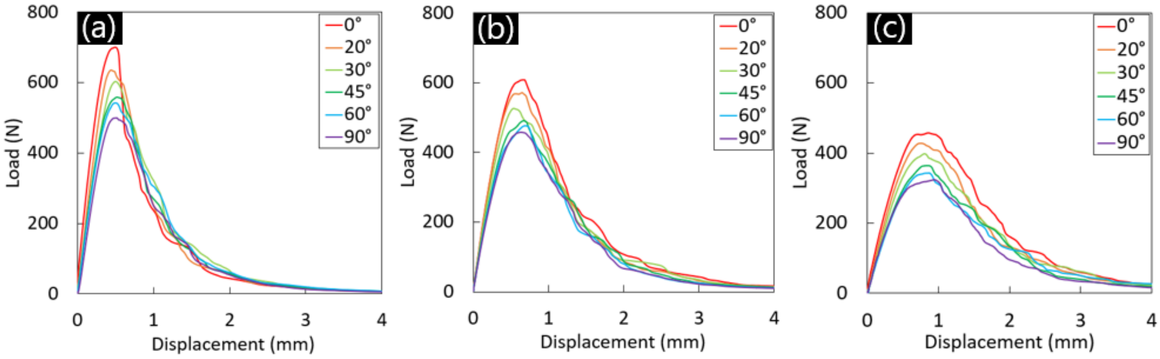

Figure 4: Representative load-displacement curves of CT specimens tested at different machining angles and environmental conditions: (a) 23°C-DAM, (b) 23°C-RH50 and (c) 80°C-RH50.

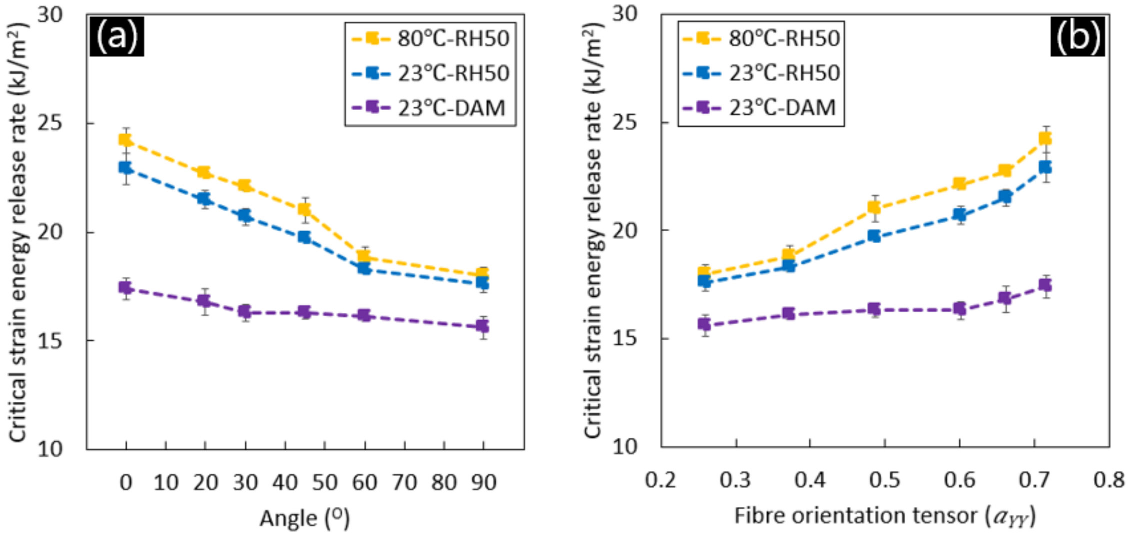

Figure 5: Fracture toughness of PA66-GF50 material as a function of machining angle (a) and fibre orientation tensor a_{YY} (b), under different environmental conditions.

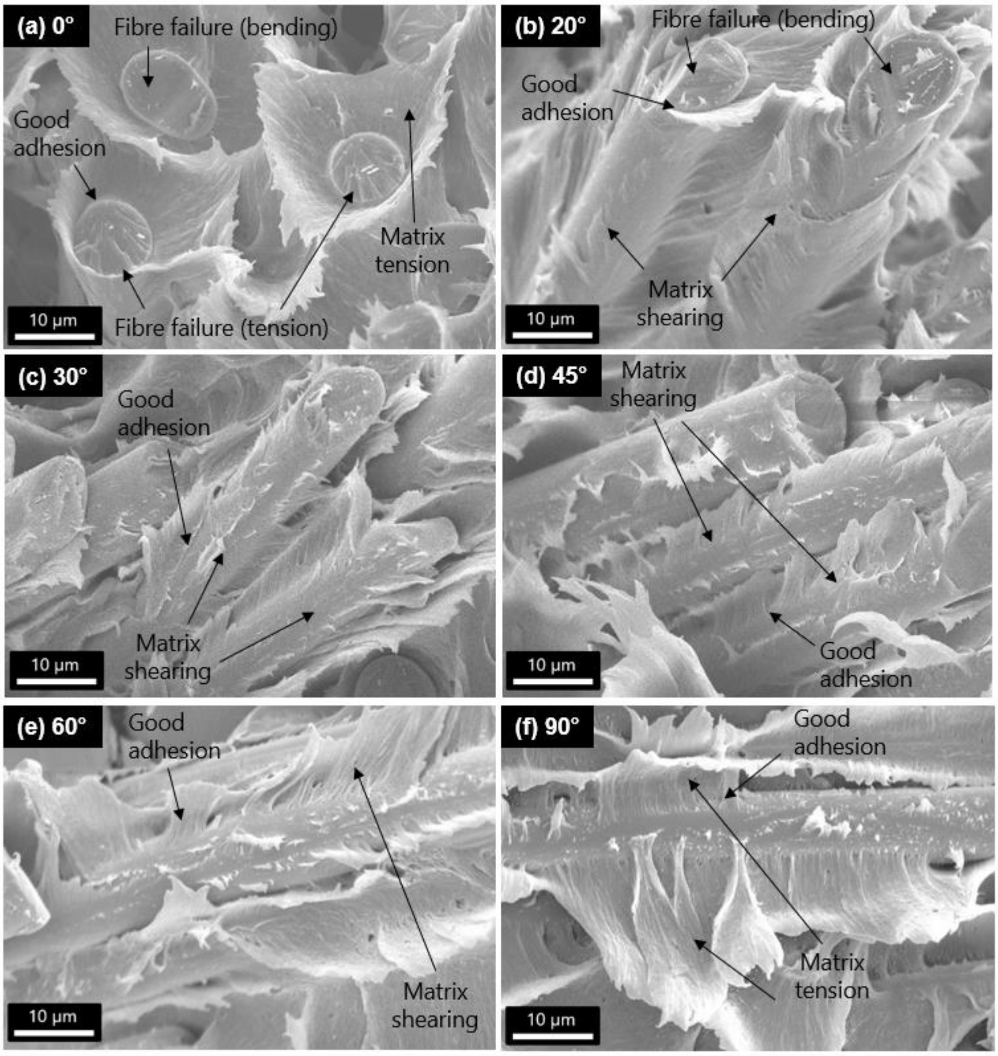

Figure 6: Electron micrographs of the fracture surfaces of CT specimens (in shell region) after testing at 23°C-DAM conditions: (a) 0°, (b) 20°, (c) 30°, (d) 45°, (e) 60°, (f) 90°.

4 TESTING OF SUB-COMPONENTS

PA66-GF50 subcomponents were tested under quasi-static conditions at 23°C and 80°C, and under DAM or RH50 conditions. During the testing, the load (P) was applied through continuous quasi-static displacement control of the indenter along the negative *B* direction in Figure 3.

Figure 7 (a) shows the load-displacement curves of subcomponents under the three different environmental conditions. Softer behaviour was observed under wetter or hotter conditions. The crack initiated at the opposite face of the loading point, then it propagated along the *B*-*C* plane, as shown in Figure 7 (b). This crack propagation direction and the fracture plane were consistently observed for all the tested subcomponents regardless of the environmental conditions.

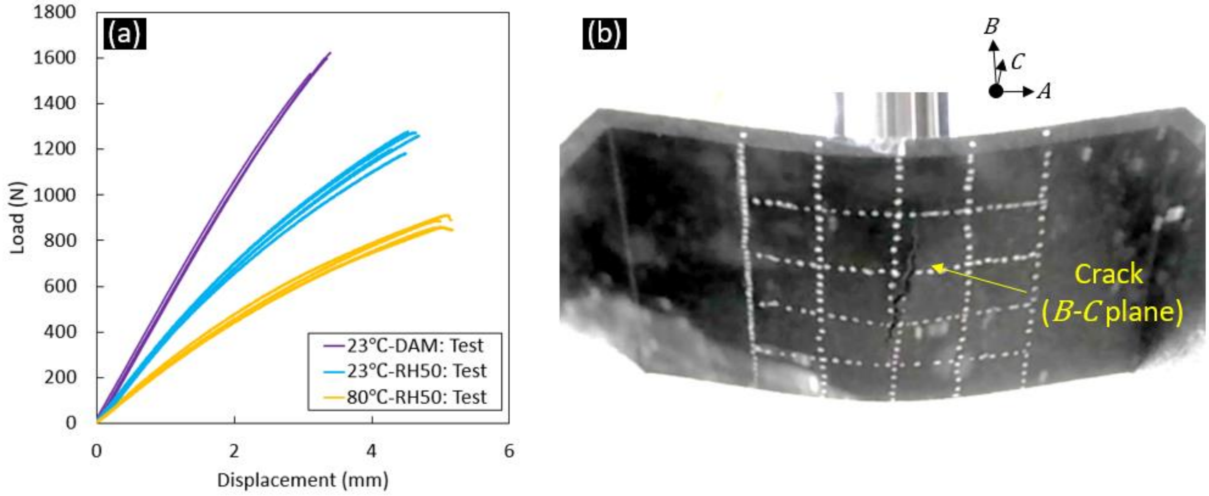

Figure 7: (a) Load-displacement curves of subcomponents under different environmental conditions, and (b) photograph of subcomponents during the test.

5 SIMULATIONS OF SUBCOMPONENTS

Moldflow software [4] was used to simulate the injection-moulding process and to predict the fibre orientation in the subcomponents. The fibre orientation tensor was then mapped onto an Abaqus [5] Finite Element Analysis (FEA) model of the subcomponent under quasi-static indentation, using Digimat-MAP [6].

The PA66-GF50 material was modelled using Digimat's elastic-plastic material model (based on orientation averaging [7], Mori-Tanaka/Voigt mean-field homogenization [8] and J_2-plasticity model [6]), calibrated with the dog-bone tensile testing data under several machining angles, accounting for the anisotropy and material nonlinear-response. We present full details of these coupled process/structural simulations ("coupled FEA") elsewhere [9].

Figure 8 shows load-displacement curves obtained experimentally or from the coupled FEA, using two approaches to predict failure:

- The conventional approach: failure initiation predicted by the Tsai-Hill ("TH") criterion [1, 6]. The failure point corresponds to the moment when the Tsai-Hill failure criterion is first met.
- Accounting for the fracture toughness of the material: by using the CT test results (Figure 5) as inputs for cohesive zone modelling ("CZM"), mapped according to the complex core-shell fibre orientation states predicted by the process simulation (details are shown in [9]).

A good agreement was observed regarding the initial stiffness and progressive softening in all simulation results. However, the FEA with the TH criterion predicted onset of failure about 20% earlier than the failure point observed in the tests under all environmental conditions. These results clearly demonstrate that the failure models currently implemented in commercially-available software, based on failure initiation criteria, are not sufficient to accurately predict the maximum load in the tests.

To improve failure predictions, the finite fracture toughness of the material (Figure 5) was then introduced in the simulations (in the “FEA (CZM)” approach). This approach showed excellent agreement of the failure points between the simulations and the test results, within less than 3% error in the failure load for all environmental conditions. This demonstrates that accounting for the finite fracture toughness of the material is essential to accurately predict the failure load of IM-SFRP components.

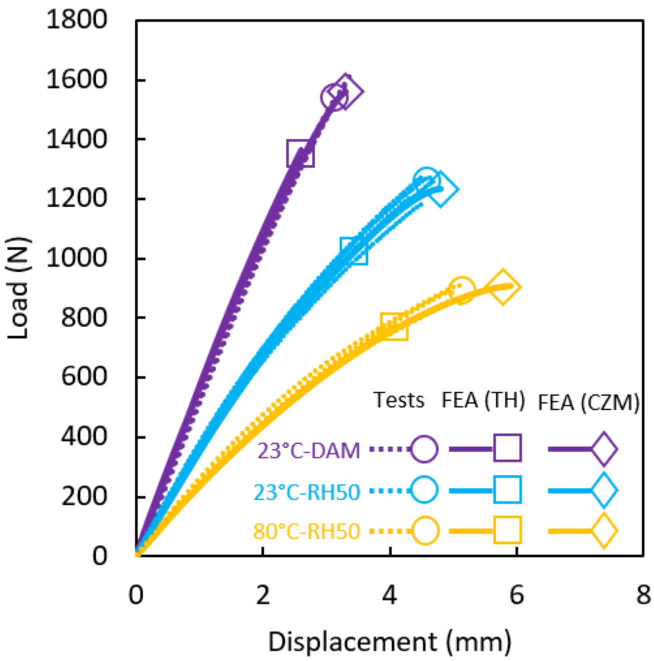

Figure 8: Load-displacement curves of subcomponents from tests and simulations under different environmental conditions.

6 CONCLUSIONS

PA66-GF50 composite coupons and subcomponents were tested under different environmental conditions; coupled process/structural simulations using CZM calibrated with measured fracture toughness showed excellent agreement of failure points with the test results (within 3% error). This work demonstrates that accounting for the finite fracture toughness of IM-SFRPs is required to overcome the limitations of conventional methodologies, and accurately predict the ultimate failure of components.

ACKNOWLEDGEMENTS

This research was funded by Asahi Kasei Corporation under the “Material Modelling of Short-Fibre Reinforced Composites” project.

REFERENCES

[1] E. Kurkin, M. Spirina, O. Barcenas, E. Kurkina, Calibration of the PA6 short-fiber reinforced material model for 10% to 30% carbon mass fraction mechanical characteristic prediction, *Polymers*, **14**, 2022, 1781.

[2] Y. Fujita, S. Noda, J. Takahashi, E.S. Greenhalgh, S. Pimenta, Initiation and propagation fracture toughness of injection-moulded short fibre composites under different environmental conditions, *Composites Science and Technology*, **233**, 2023, 109891 (doi.org/10.1016/j.compscitech.2022.109891).

[3] BS EN ISO 1110:2019 Plastics - Polyamides - Accelerated conditioning of test specimens.

[4] Autodesk. Moldflow. Plastic injection and compression mould simulation for design and manufacturing (https://www.autodesk.co.uk/products/moldflow/overview, accessed on April 24th 2023).

[5] Dassault Systemes. Abaqus Analysis User's Guide Version 6.14.

[6] e-Xstream engineering. Digimat 2022.2 user's documentation.

[7] S.G. Advani, C.L. Tucker, The use of tensors to describe and predict fiber orientation in short fiber composites, *J. Rheol*, **31**, 1987, 751–784.

[8] T. Mori, K. Tanaka, Average stress in matrix and average elastic energy of materials with misfitting inclusions, *Acta Metall*, **21**, 1973, 571-574.

[9] Y. Fujita, S. Noda, J. Takahashi, E.S. Greenhalgh, S. Pimenta, Combining fractography, fracture mechanics and FE modelling to improve the failure prediction of injection-moulded short fibre composite components, manuscript under preparation (2023).